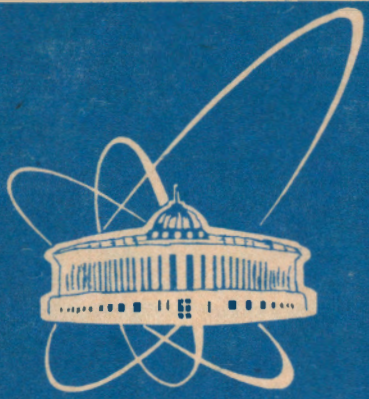

СООБЩЕНИЯ
ОБЪЕДИНЕННОГО
ИНСТИТУТА
ЯДЕРНЫХ
ИССЛЕДОВАНИЙ

Дубна

E3-95-304

V.L.Aksenov, N.N.Isakov, R.M.A.Maayouf*

THE NSKAT NEUTRON SPECTROMETER FOR QUANTITATIVE TEXTURE ANALYSIS (NSKAT Project)

*Reactor and Neutron Physics Department, NRC, Atomic Energy Authority, Cairo, Egypt

1995

Аксенов В.Л., Исаков Н.Н., Мааюф Р.М.А. Е3-95-304

Нейтронный спектрометр для количественного анализа текстуры (Проект НСКАТ)

Предложена конструкция нейтронного спектрометра для постановки современных нейтронографических методик анализа текстур материалов и программа физических и прикладных исследований.

Работа выполнена в Лаборатории нейтронной физики им.И.М.Франка ОИЯИ.

Сообщение Объединенного института ядерных исследований. Дубна, 1995.

1. Introduction

For over seventy years textures of different materials have been intensively studied [1,2]. This research direction is of great interest to the development of methods for building materials with a given complex of properties, as well as to the theory of plastic deformation. The presently existing theories of texture formation and evolution processes, which make up the physics and mechanical basis of methods for the production of materials with a given anisotropy of properties are not precise, and demand a new input of higher precision experimental data.

Different experimental methods of texture analysis have been elaborated [1,2]. Each method has its optimal fields of application.

The method of neutron diffraction, in combination with the time-of-flight method, has considerable advantages over other methods for investigating textures. First, the high neutron penetration depth provides a means for obtaining direct information about the distribution of preferred orientations of crystallites (grains) in an investigated sample without destroying it. To compare the possibilities of neutron and X-ray diffraction methods, we should note only that gamma-rays can penetrate to a depth of 0.3 mm, and neutrons to a depth of 50 mm and deeper. Second, all possible Bragg reflection peaks from the investigated sample are measured simultaneously in every time-of-flight spectrum, provided the primary neutron beam has a sufficient range of wavelengths. The latter raises the efficiency of texture investigations, especially of the textures of inhomogeneous multi-phase materials with low crystallographic symmetry. As a result, the areas for the application of neutron diffraction to the solution of fundamental and applied problems expands without limit.

The Frank Laboratory of Neutron Physics of the Joint Institute for Nuclear Research has much experience in investigating textures with the NSVR high resolution neutron spectrometer, whose physical and technical characteristics are described in [3]. Since the NSVR startup in 1989 on channel 7A at the IBR-2 reactor the scope and number of proposals for experiments utilizing it has been increasing in an avalanche manner in spite of the fact that texture analysis in its present state is a labor consuming process demanding large time expenditures for both staging an experiment and processing the obtained data. A NSVR experiment to measure diffraction spectra from a sample takes an average of 30 hours, yet during one reactor year about 100 samples are measured with NSVR. This is a very large measurement-carrying capacity in comparison to other analogous instruments.

The NSVR spectrometer operates in a user mode for specialists in many fields of science where a knowledge of textures is necessary. It should be noted that their close cooperation mediates a quick mastery of the investigation results. The growing user demand for beam time could be met by building several more texture spectrometers and co-ordinating a joint scientific research program.

The aim of this paper is to propose a project of constructing a physical instrument for developing up-to-date procedures of carrying out experiments for the investigation of textures of different materials by the neutron diffraction method. The present paper is the result of discussions of texture investigation programs which considered the possibility of staging such experiments on one of the neutron beams of the ET-RR-1 reactor of the Atomic Energy Authority of Egypt or at a higher power reactor.

The work is being carried out under the auspices of the Agreement for scientific and technical cooperation between AEAE and JINR.

The present proposal is an updated version of the proposal described in [4], and it takes into consideration the experience of investigations carried out since the time of the first proposal and includes the plan for upgrading NSVR to meet the new requirements for precision and completeness of experimental data for quantitative texture analysis. Here, it should be noted that NSVR still retains the world leading position in neutron flux and quality of obtained experimental information, as well as in the spectrum of texture problems that could be solved with its help [5,6,7].

2. Theoretical background

Texture is the presence of a preferred orientation of separate crystallites in a polycrystal sample or molecules in a solid body in an arbitrary system of coordinates. The presence of texture in materials is demonstrated by anisotropy of their properties. In the general case, texture is described by four coordinates: three determine the orientation, and the fourth - the probability of this orientation.

There exist four main methods of classifying textures [2]:

1. Method of ideal orientations.
2. Classification by process types, e.g., forging texture, recrystallization texture, etc.
3. Unitary texture classification on the basis of the theory of symmetry.
4. Texture classification based on reconstruction, analysis and classification of orientation distribution functions (ODF) of crystallites in a sample. This last method is now considered optimal.

Today, the general requirement is that all methods of texture analysis should provide exact quantitative information.

The method of analysis based on the calculation of ODF gives a complete texture description. This method allows one to describe unambiguously the texture of a certain crystal phase, p, in a sample.

$$f^p(g) = \frac{dV^p(g \in dg)}{V^p} dg \geq 0, \tag{1}$$

where $f^p(g)$ is the ODF, and

$$\oint_G f^p(g) dg = 8\pi^2 \tag{2}$$

determines the volume portion of all crystallites in the p phase with the orientation

$$g = \{\alpha, \beta, \gamma\} \in dg \tag{3}$$

in the orientation space

$$G : 0 \leq \alpha, \gamma < 2\pi, 0 \leq \beta \leq \pi. \tag{4}$$

This procedure is described in a greater detail in [8].

Theoretical methods do not permit one to calculate the anisotropy of polycrystal materials. One needs to have experimental data on ODF which cannot be measured directly. Experimental data provides a means for constructing pole figures (PF) which are then used to calculate the ODF. A pole figure is a graphic image on the stereographic projection of the distribution function of normals onto a definite crystallographic plane (hkl). The pole figure gives the complete characteristic of the texture, provided the orientation packing density is

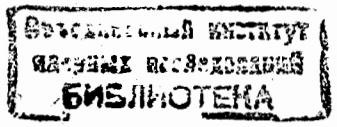

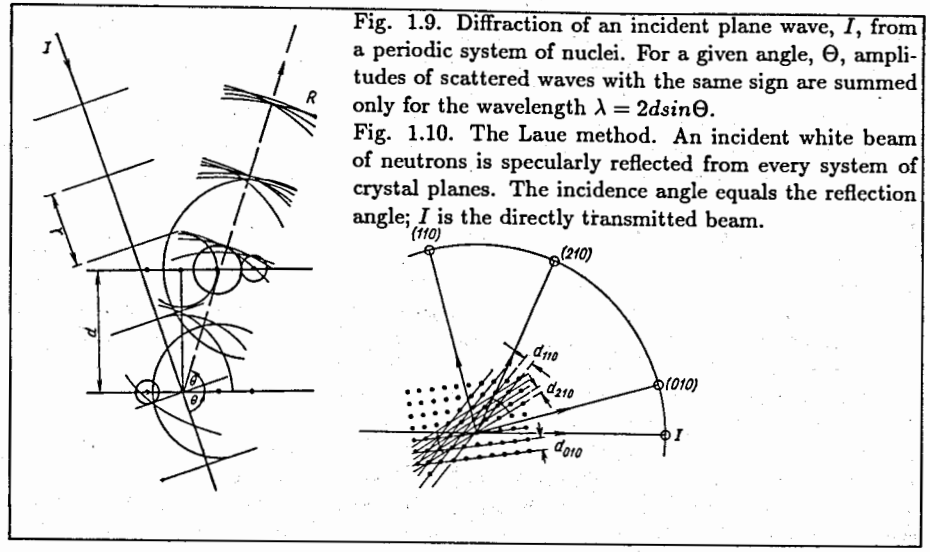

Fig. 1.9. Diffraction of an incident plane wave, I, from a periodic system of nuclei. For a given angle, Θ, amplitudes of scattered waves with the same sign are summed only for the wavelength $\lambda = 2dsin\Theta$.

Fig. 1.10. The Laue method. An incident white beam of neutrons is specularly reflected from every system of crystal planes. The incidence angle equals the reflection angle; I is the directly transmitted beam.

Fig. 1. Interference following neutron beam scattering.

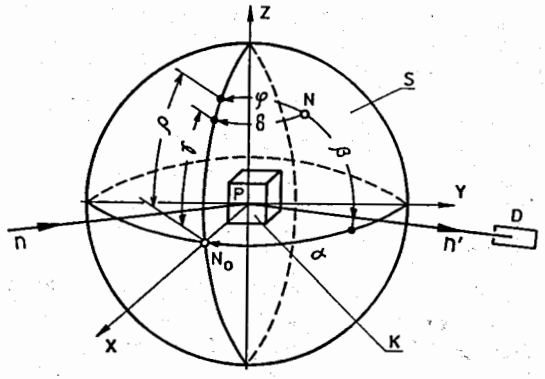

Fig. 2. The scheme illustrating how sample texture can be measured by the diffraction method with one detector. The scheme shows all possible rotation angles to place the normal to the plane of an arbitrary grain in the reflecting position. D is the detector, n is the primary neutron beam, n' is the reflected neutron beam.

indicated for each point of the projection plane, i.e., the relative or absolute number of exits of normals towards the (hkl) plane is indicated. This number is the measure of the pole density. The pole density is proportional to the reflected neutron beam intensity.

The quantitative texture analysis of large volumes (several cm^3) of inhomogeneous polycrystal materials can be carried out only with the help of the neutron diffraction method of measuring pole figures.

3. The method of neutron diffraction experiments to determine the texture of a sample. The physical and methodological background of the NSKAT project

In recent years the use of neutron diffraction applications to study material textures has constantly been expanding. This method permits the structure of the atomic lattice and its orientation to be determined in large volume samples without destroying them (non-destructive testing).

The diffraction determination of crystal structures is based on fulfillment of the Bragg-Wolf condition:

$$n\lambda = 2d_{hkl} \times sin\Theta, \tag{5}$$

where λ is the neutron wavelength, d is the atomic lattice interplane spacing, Θ is the reflection angle, n is the positive integer called the reflection index.

For illustration, the interference patterns arising upon the scattering of a neutron beam on a periodic structure with a d period are shown in fig. 1 (figs. 1.9 and 1.10 in [9]). According to eq.(5) each d period causes scattering at a definite angle for every given wavelength.

The time-of-flight method permits determining the wavelength of neutrons reflected at a given angle during the registration time:

$$\lambda = \hbar t/mL \tag{6}$$

$\hbar = 6.62618 \times 10^{-34} J/sec$ is Planck's constant;
$m = 1.67495 \times 10^{-24} g$ is the mass of the neutron.

By measuring the time,t, (in μsec) in which a neutron flies the distance, L,(in mm) we obtain the wavelength λ (in nm):

$$\lambda = 0.3956t/L, \tag{7}$$

Earlier, it was said that we obtain data for constructing PF from the experiment. To meet this aim, either the sample or detector should be successively turned to have any of the directions in the sample in a position to reflect neutrons into the detector (see fig.2). Figure 2 shows a spherical sample,S, in the centre of which one of the crystallites, K, is placed. The figure gives all possible rotation combinations by which a normal to the P plane of this grain, earlier orientated towards the N point on the spherical surface, can be reorientated in the direction of the X axis (the N_o point on the spherical surface). As a result, the P plane would be in a position to reflect neutrons into the D detector. It is clear that rotation of the sample about the X axis will not change the geometrical conditions of reflection from this plane. It is obvious that to find all possible reflecting planes in the sample volume one has to use rotation combinations about different axes. The choice of combinations depends on the conditions of a concrete experiment: the necessary scanning net density, number of detectors, their arrangement scheme, sample orientations with respect to the detectors system. By

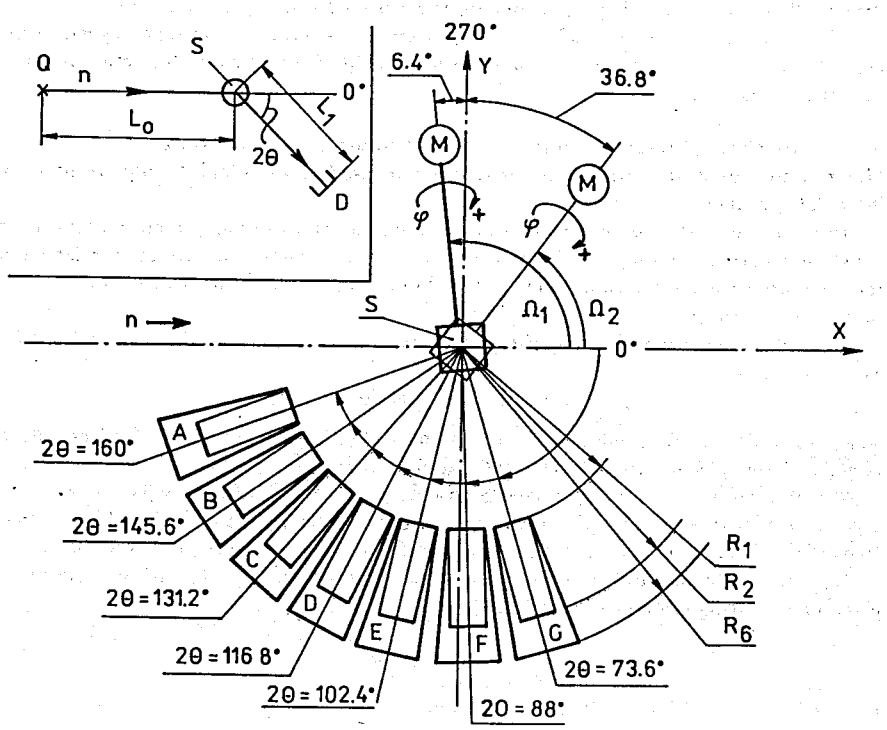

Fig. 3. Schematic of the detector system and sample arrangement with respect to the neutron beam axis for measuring complete PF on NSVR. The XY-plane is located horizontally. The rotation directions of the S sample by the ϕ and Ω angles are indicated. The centre of the sample is in the geometrical centre of the detector system. The directions for counting out the 2Θ angles are shown. The main dimensions of the instrument: R_1=986 mm is the distance from the geometrical centre of the detector system to collimators' entrance windows; $R_2 = L_1$=1600 mm is the distance to the centre of the detector batteries; R_6=2000 mm is the maximal size of the platform. L_0=103.4 m is the distance from the centre, Q, of the reactor core to the geometrical centre of the detector system.

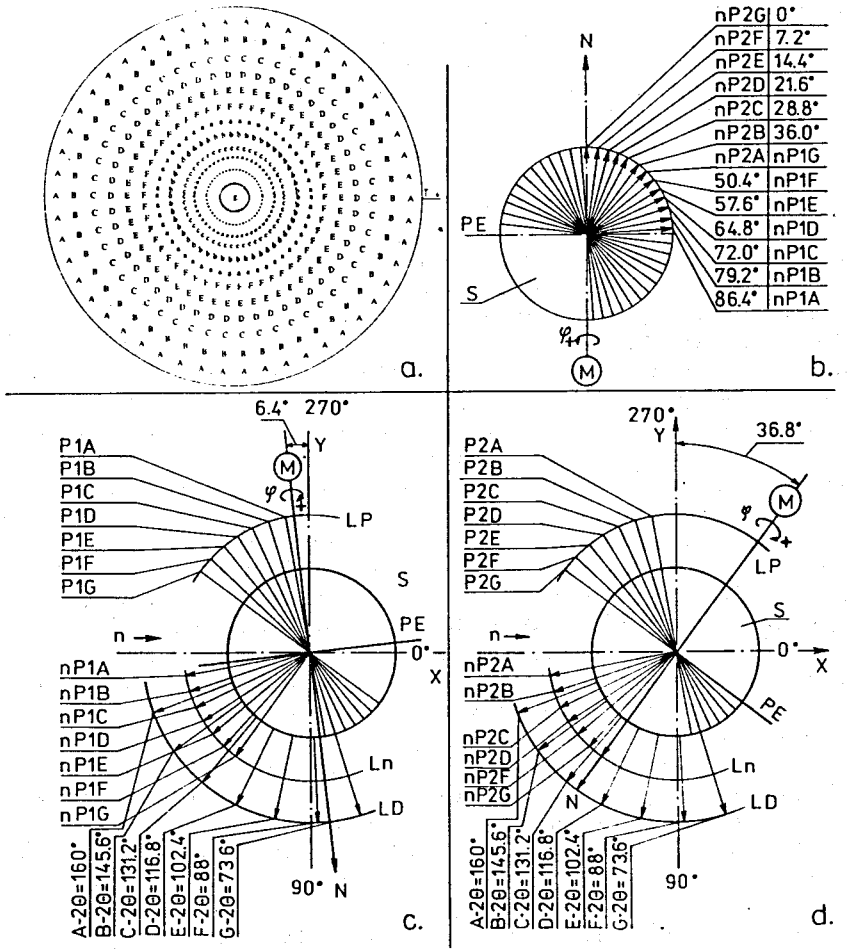

Fig. 4. The detailed scheme of the experiment to measure textures of samples on NSVR with the regular scanning net density of 7.2° × 7.2°; (a) raster of the total pole figure; (b) - scheme for interpreting the raster points in the system of coordinates related to the sample, the g zone indicated in the centre of the raster corresponds to the direction of $nP2G$ normals towards the $P2G$ plane; (c) and (d) - schemes for measuring the inner and outer sides of the pole figure.

moving the sample in a proper manner, all orientation planes (hkl) available in the sample can be made to occupy the reflecting position in turn. In the process, the reflection intensity, i.e., the scattering cross section is measured. The intensity is the measure of the density of filling the given orientation by corresponding lattice planes. On a single pole figure only one type of crystal planes can be pictured.

Figure 3 shows the scheme of the experiment most often used on the NSVR spectrometer to measure the texture of a sample, S. This is the optimal scheme for NSVR. The maximal positioning density of the detectors is 14°. The dimensions of the ring sector (the 116° platform for positioning detectors) allow the positioning of 8 detectors. Unfortunately, the registration equipment made in CAMAC standard, because of the accepted ideology of information processing at the time of NSVR's construction, does not permit the processing of information from a larger number of detectors without an essential loss in the quality or time of data collecting.

A denser scanning net can be achieved with NSVR, e.g., $3.6° \times 3.6°$. To have an even higher scanning density, the whole detector platform could also be turned 7.2° with respect to its position shown in fig. 3. This would double the number of positionings related to the ϕ angle. The measuring time would then be increased by four times.

It would make no sense, however, to use a higher density scanning net in NSVR experiments, because the structure of the used soller collimators, which permits the beam angular divergence into the 2Θ scattering angle to be limited to 1°, in the vertical plane, allows the divergence of 6°. The size of the collimators, i.e., their length (for a given uncertainty of the 2Θ angle in the scattering and in the transmission plane), the cross section area (depending on sample dimensions or the cross section diameter of available neutron beams), and the number of collimators, mainly determine the size of the instrument. The measuring time for a given scanning net density and neutron flux density on the sample per unit of time depend on the number of collimators. Modern technology provides a means for constructing new soller collimators which would permit reducing the size of instruments for neutron texture analysis. A decrease in the $R2$ distance would not only reduce the size of the instrument but would also raise the density of the registered flux of scattered neutrons in inverse proportion to the square of its decrease and reduce the time expenditure for the experiment.

Figure 4a presents the total pole figure raster obtained in the experiment whose scheme is shown in fig. 3. Figures 4b,c,d detail the experimental procedure and interpretation of the experimental results in further mathematical processing.

Ln is the line of exits of normals in the direction of the corresponding planes, e.g, the $nP2G$ normal is the normal to $P2G \equiv PE$. LP is the line of plane exits; only planes transversing the centre of the S spherical sample are shown. LD is the line of direction pointer exits in the direction of the soller collimators of the corresponding detectors. The PE plane is the equatorial plane of the S sample in the system of coordinates related to the sample. N is the north pole of the sample. The step-driver, M, rotating the sample by ϕ angles is positioned at the south pole end of the sample. As it can be seen from the Table in fig. 4b summarizing the normal exit angles in the sample system of coordinates, points on the normal exit belt $nP2_iA(i = 0,...,49)$ are measured twice in the present scheme of conducting experiments, i.e., measurements in the $nP2A$ and $nP1G$ belts must be identical. This little trick permits sewing up the inner and outer sides of the pole figure in the data processing. To do this, the A and G detectors should be absolutely identical, but, in practice, one has to introduce

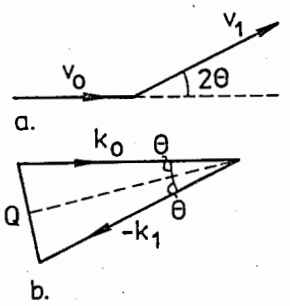

Fig. 1.7. Elastic scattering in real (a) and inverse (b) space. The vectors are related as $mv = \hbar k$. In elastic scattering, $| k_o | = | k_1 |$, and the scattering angle in inverse space is therefore is an isosceles triangle and $Q = 2k_o sin\Theta$.

Fig. 1.8. The Q value achievable for a given wavelength and scattering angle. For a given wavelength the scanning over all angles corresponds to Q changing in a limited interval. Wavelength scanning at a fixed angle corresponds to the interval of Q changes determined by the wavelength interval.

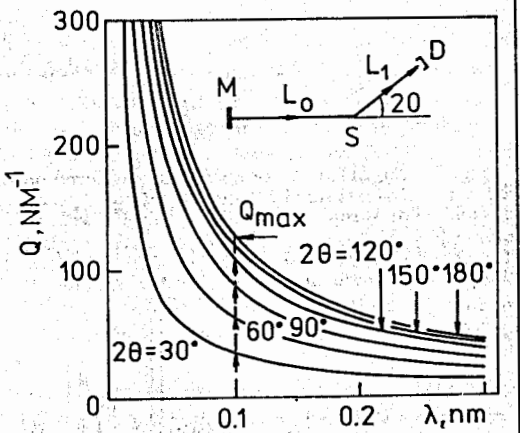

Fig. 5. The scheme to explain the difference in scattering geometries and the dependence of the Q value on the wavelength and scattering angle.

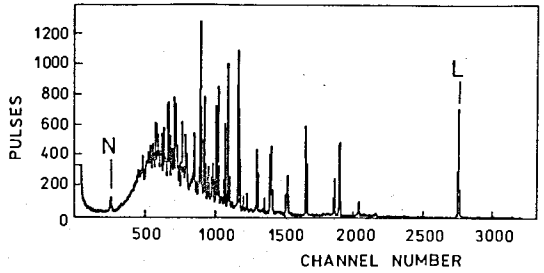

Fig. 6. The instrumental spectrum MDOL.a00 measured with the NSVR spectrometer of FLNP JINR on May 21, 1991. The sample is a Mongolian dolomite cube with a side of 30 mm and a volume of $V = 27\ cm^3$. The A detector: the angle $2\Theta = 160°$, the time channel width $\Delta\tau' = 64\mu sec$, and the exposition time, 15 min. The IBR-2 reactor operation mode - pulsed - with a frequency of 5 Hz at a mean power of 2 MW.

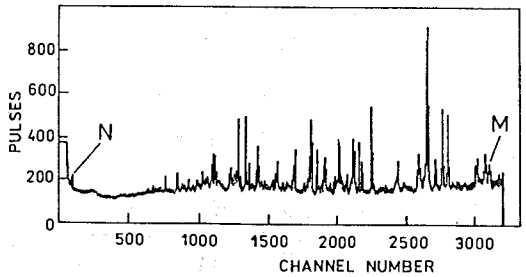

Fig. 7. The SI1SI1A.nor spectrum measured on the NSVR spectrometer of FLNP JINR. The curve was obtained by mathematically processing the experimental data of February 18, 1992. The sample is the SI1SI cylinder with a diameter of 30 mm, height=30 mm, and volume $V = 21.2\ cm^3$. The A detector: the angle $2\Theta = 160°$, the time channel width $\Delta\tau' = 64\ \mu sec$, and the exposition time, 15 min. The IBR-2 reactor operation mode - pulsed - with a frequency of 5 Hz at a mean power of 2 MW.

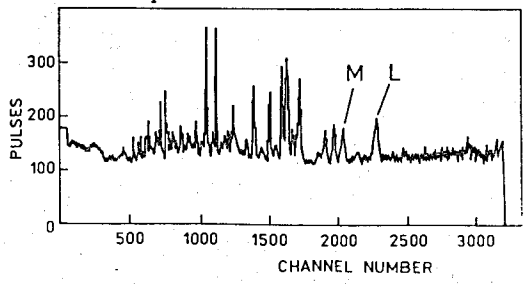

Fig. 8. The SI1SI1G.nor spectrum measured on the NSVR spectrometer of FLNP JINR. The curve was obtained by mathematically processing the experimental data of February 18, 1992. The sample is the SI1SI cylinder with the diameter of 30 mm, heght=30 mm, and volume $V = 21.2\ cm^3$. The G detector: the angle $2\Theta = 73.6°$, the time channel width $\Delta\tau'$=64 μsec, the exposition time is 15 min. The IBR-2 reactor operation mode - pulsed with a frequency of 5 Hz at a mean power of 2 MW.

corrections. Difficulties in data processing are also caused by the positioning of detectors in different Debye-Scherrer cones and by different experimental geometries necessary for different detectors. Each detector has its own scattering vector (Q-vector) equal to:

$$Q = k_0 - k_1, \tag{8}$$

and for the elastic scattering at an angle 2Θ, it is equal to:

$$Q = 2k_0 sin\Theta = 4\pi sin\Theta/\lambda_0. \tag{9}$$

For details see fig. 5 (figs. 1.7 and 1.8 in [9]).

The detectors A, B, C, D, E operate in the reflection geometry, and the detectors F and G in the transmission geometry. This necessitates introduction of separate corrections for each detector. Experimental data correction and refining are inevitable. For example, it is necessary to introduce corrections for the size and shape of the sample. It is therefore better to use samples of standard size and shape (sphere, cube, cylinder). Spherical samples are ideal for neutron texture analysis because, first, the length of the neutron path in the volume of a spherical sample does not depend on its orientation angle with respect to the primary neutron beam and each of the detectors. Second, a sphere has a larger volume than any other spatial form for the same maximal linear dimensions. The use of spherical samples might therefore reduce not only the measuring time but also the instrument's dimensions. For example, from the viewpoint of material's presentation an optimal size for rock samples appeares to be a volume from 20 to 30 cm^3. The diameter of a 30 cm^3 sample is not less than 4 cm, and the spatial diagonal of a 27 cm^3 cube is equal to about 5.2 cm. In practice, we have to work with cylindrical or cubic samples because they are easier to produce.

The NSVR experiments for measuring textures of rock samples have demonstrated that the achieved NSVR resolution

$$R_d = \Delta d/d = \Delta\lambda/\lambda \tag{10}$$

(for an inter-plane spacing $d = 2\AA$ and the detector positioned at the angle 2Θ=160° and R_d =0.004=0.4%, 2Θ=90° and R_d=0.007=0.7%, and 2Θ=73.6° and R_d=0.009=0.9%), and the regular scanning net density of $7.2° \times 7.2°$ were insufficient to decode all the spectra of Bragg reflexes from geological materials, and that to have a wider working range of wavelengths would be desirable.

The R_d resolution was determined from experimental diffractograms of nickel (Ni) powder. The position (channel number) of the centre of gravity of a peak in the spectrum was calculated, i.e., the time from the moment the IBR-2 power pulse was at maximum. Then, the peak width at half maximum (number of channels) was divided by its position. Unfortunately, it is impossible to show a general method for calculating the resolution function of an arbitrary diffractometer [10]. Figures 6, 7, and 8 examplify the neutron diffraction spectra of some rock samples. These figures pictorially demonstrate a large expanse of the wavelength interval where Bragg reflexes from geological samples are located and the number of reflexes measured simultaneously.

Figure 6 presents the instrumental (without additional mathematical proccessing) time-of-flight diffraction spectrum of a dolomite sample from Mongolia. The L reflex is located in the region of inter-plane spacings d=0.336 nm=3.36 $\AA$, and the N reflex in the region of d=0.027 nm=0.27 $\AA$.

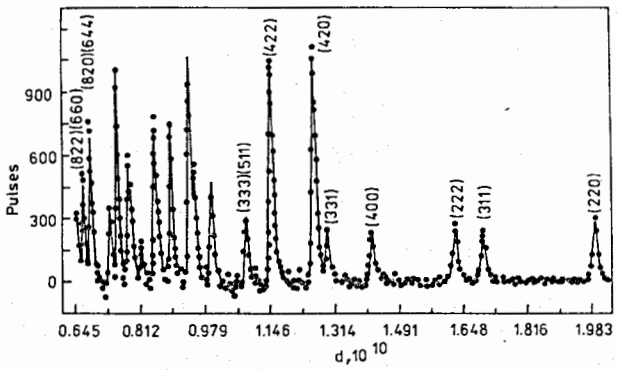

Fig. 1.11. The diffractogram of NaCl powder. The points were measured with a diffractometer at the ZINC P source of the Argonne National Laboratory, USA. The curve was obtained by mathematically processing experimental data [40].

Fig. 9.

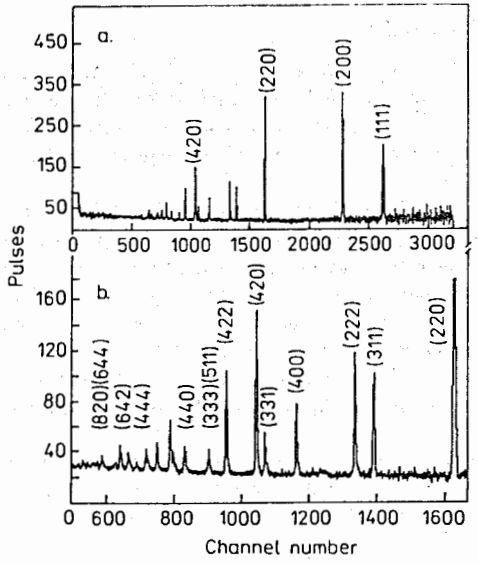

Fig. 10. The diffractogram of NaCl powder measured with NSVR of FLNP JINR in 1994. The curve was obtained by mathematically processing the data of the experiment performed on February 5, 1994. The volume of the sample was V=11.8 cm^3. Detector B: the angle 2θ=147.6°, the time channel width $\Delta\tau'$=64μsec, the exposition time, 166 min. The IBR-2 reactor operation regime: pulsed, with a frequency of 5 Hz at a mean power of 0.5 MW.

Figures 7 and 8 show diffraction spectra of the same sample measured in one experiment by detectors A and G positioned at different angles (see fig.3 and fig.4c). Attention should be paid to the fact that the wavelength range of Bragg reflexes from the sample is not completely covered by any of the detectors. The L reflex lies in the region of inter-plane spacings d=0.456 nm=4.56 $\AA$, and the N reflex in the region of d=0.0062 nm=0.062 $\AA$. To see the L reflex in the A detector spectrum (see fig.7) one should have a wider wavelength range from the primary neutron beam (up to 0.9 nm) than is currently available on NSVR (up to 0.76 nm). This can be accomplished in two ways. First, use a chopper to allow only one of every two reactor power pulses to come to NSVR. This would, however, double the measuring time. Second, switch the reactor down to the 4 Hz frequency mode. This, however, would interfere with the interests of the users working on other IBR-2 beams.

Now, let us discuss the possibility of increasing the wavelength resolution. The wavelength resolution plays an important role in decoding diffraction spectra. For comparison purposes diffractograms measured in similar experiments with different spectrometers having different resolutions and simultaneously covered wavelength intervals are given in fig. 9 (fig. 1.1 in [9]) and fig. 10. We ask the reader to pay attention to how the (331) and (420) reflexes are separated in fig. 9 and fig. 10.b showing the same section of the spectrum. There are, in addition, two more reflexes: (200) and (111), to the left of the (220) reflex in fig. 10, which are absent in fig. 3. It is easier to determine the exact position in the spectrum and, consequently, the inter-planar spacing of well separated reflexes (peaks). The low crystallographic symmetry and multi-phase composition of rocks lead to a strong superposition of Bragg reflexes. This entails strong superposition of the corresponding pole figures from which the quantitative characteristics of textures are determined. The limited possibility of separating superimposed pole figures by theoretical methods necessitates the use of a diffractometer with the highest possible resolution in the experiment [8].

The NSVR investigations of rock textures have posed new requirements for experiments:

a) a higher density scanning net, i.e., not less than 5°× 5°, and, possibly, higher;

b) a wavelength resolution on the level of $5 \times 10^{-4} - 5 \times 10^{-5}$.

Having a good resolution permits expanding the research program carried out with the spectrometer. For example, information about internal stresses in an arbitrary region of a sample could be obtained by analysing peak shape in the spectrum. One might achieve a higher resolution on channel 7A by installing a chopper to cut a very narrow part of the pulse at maximum power, but this would, however, lead to an essential increase in measuring time. Other ways exist to achieve good resolution, but the cost is always high, particularly, when it involves the reconstruction of an existing channel. It is advisable that the project of a channel for texture investigations would be elaborated, considering the necessary resolution. With the startup of the new nickel movable reflector at IBR-2 the resolution of channel 7A will increase by a factor of 1.5.

The above detailed discussion of experimental techniques and difficulties in texture investigations with NSVR is necessary to clearly understand the ideas that form the basis of the SKAT and NSKAT projects. The SKAT project [4] solves the problem of increasing the scanning density net and simultaneously reducing the measuring time and the number of corrections necessarily introduced into experimental data by more conveniently positioning the detector system for texture analysis purposes.

The SKAT project also uses the recently found possibility of reducing the size of the

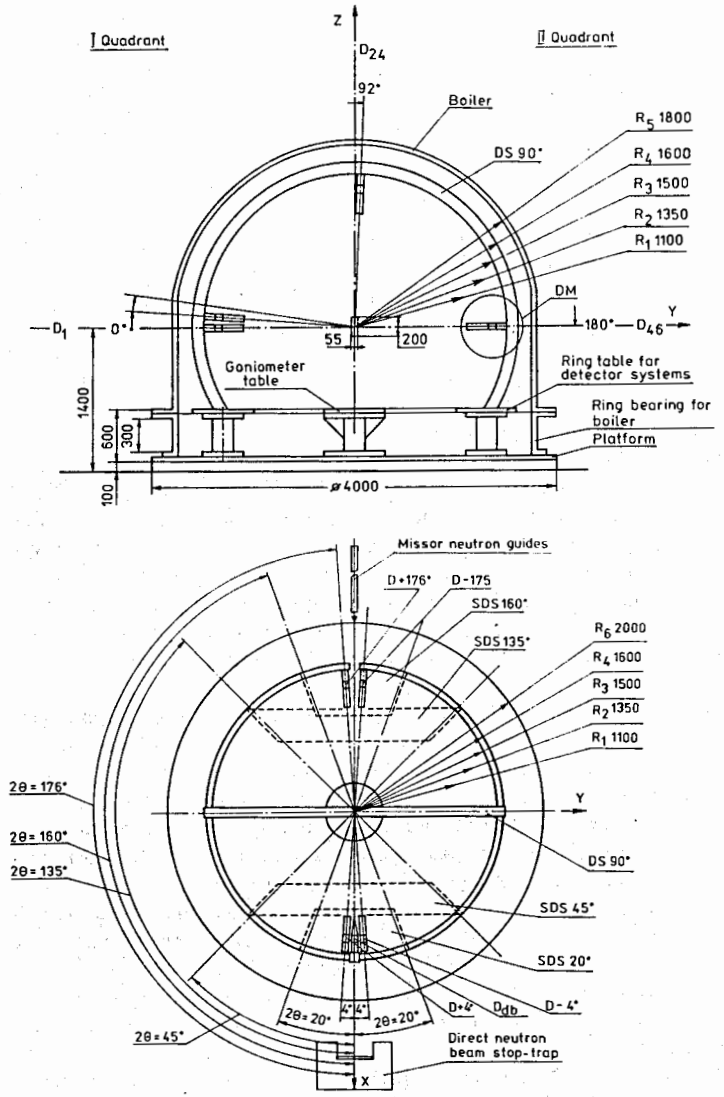

Fig. 11. A schematic of the NSKAT-55-4 neutron spectrometer.

instrument by introducing the new soller collimators - the foil soller collimators (FSC) with a gadolinium (Gd) covering layer. The R_2 distance would be reduced to 1000 *mm* (fig.3). This possibility could not be included in the earlier project [4]. Because of the limited space between the 7A beam axis and the floor of the experimental hall, the rated maximum density of positioning detectors, 5°, will not, however, be achieved, and it will be 5.6°. This does not mean that the scanning net density cannot be higher. This issue has been discussed above. The SKAT facility will have 64 detector modules positioned on a 360° ring lying in a plane at the scattering angle $2\Theta = 90°$. This will give the possibility of using scanning nets of up to 1.4°× 1.4° for measuring incomplete pole figures during minimum measuring times.

4. The NSKAT project

The NSKAT project does not have the limitations and disadvantages of the SKAT project because it assumes adjusting the beam to the spectrometer, not the spectrometer to the beam.

The instrument is to be developed and constructed to solve a definite sphere of problems. The NSKAT instrument (fig. 11) would provide the possibiltiy of staging experiments that satisfy today's requirements for precision and completeness of experimental information for the texture analysis of materials in:

1. Investigating textures of natural geomaterial samples (for the present, we are speaking about rock samples only).

2. Investigating the dynamics of changes in textures of metal and metal alloy samples caused by external conditions which modify the textures while in the neutron beam. External stresses in the textures could be also investigated in a simultaneous or parallel mode.

3. Carrying out the same as in no.2 investigations with polycrystal, ceramic, and polymer samples of artificial origin (homogeneous in composition).

4. Measuring textures of HTSC-materials to enhance HTSC producing technologies. (A proposal with a program of such measurements has been submitted to FLNP. This program would take from three to five years of the NSVR time).

5. Investigating textures of biological samples.

5. The NSKAT design

The texture spectrometer schematically shown in fig. 11 would permit carrying out the experimental programs outlined in Section 4. Its design assumes the use of a neutron beam with a cross section diameter of 55 *mm*. Such a diameter is needed for a cubic sample with a side of 30 *mm* to be totally immersed in the beam regardless of the sample's orientation with respect to the beam. The detector system DC90° is positioned in the ZY vertical plane perpendicular to the incident beam. The 2Θ scattering angle for all detectors in the system is the same - 90°. On a half 0° to 180° ring a maximum of 45 detector modules (*DM*) can be located with a density of 4°. The *DM* detector module consists of a collimator, a detecting chamber, and an adjusting device. In the four horizontal sectors of the *XY* plane, detector modules of the same size can also be positioned with the same density. In fig. 11 the DM's positioned in the *XY* plane sectors at the edge sites D±4° and D±176° are shown in addition to the Dnn direct beam detector. For example, for a primary neutron beam with a wavelength interval from 0.06 to 10 Å the planar spacings d=0.042 - 7.071 Å would be feasible for the DC90° detector system, d=0.86 - 143.27 Å for the D±4°, and d=0.03 -5.0 Å for the D±176°. The spectrometer's dimensions permit one to position any device for creating

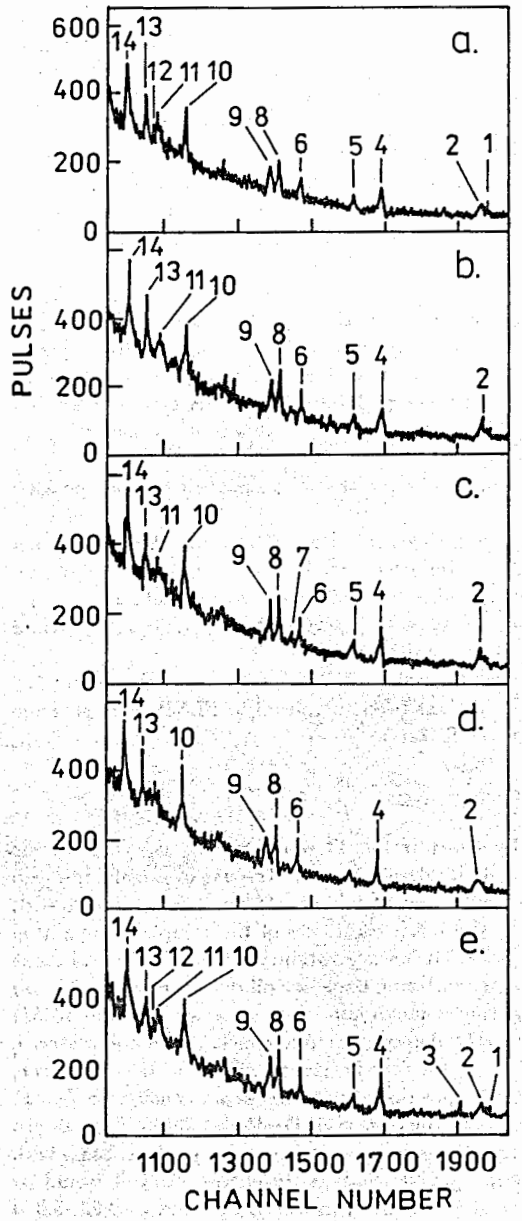

Fig. 12. The diffractograms of the sample of a $YBa_2Cu_3O_{7-\delta}$ HTSC material from WTSP2AX experiment of February 2, 1992 performed with NSVR of FLNP JINR. The sample is a cylinder with a diameter=8 *mm*, height=10 *mm*, volume V=0.50 cm^3, and the exposition time, 180 *min*. The time channel width is $\Delta\tau'$= 64μsec. The D detector: 2θ=116.8°, scanning is by the Ω angle with a step of 1.8 ° (see fig. 4).
(a) the wtsp2.d05p spectrum, Ω = 299.6°;
(b) the wtsp2.d06 spectrum, Ω = 301.4°;
(c) the wtsp2.d07 spectrum, Ω = 303.2°;
(d) the wtsp2.d08 spectrum, Ω = 305°;
(e) the wtsp2.d09 spectrum, Ω = 306.8°;
The IBR-2 reactor operated in the pulsed mode with a frequency of 5 *Hz* and a mean power of 2 *MW*.
Note that reflex (7) is seen clearly only in the (c) spectrum, and the (3) reflex in the (e) spectrum.

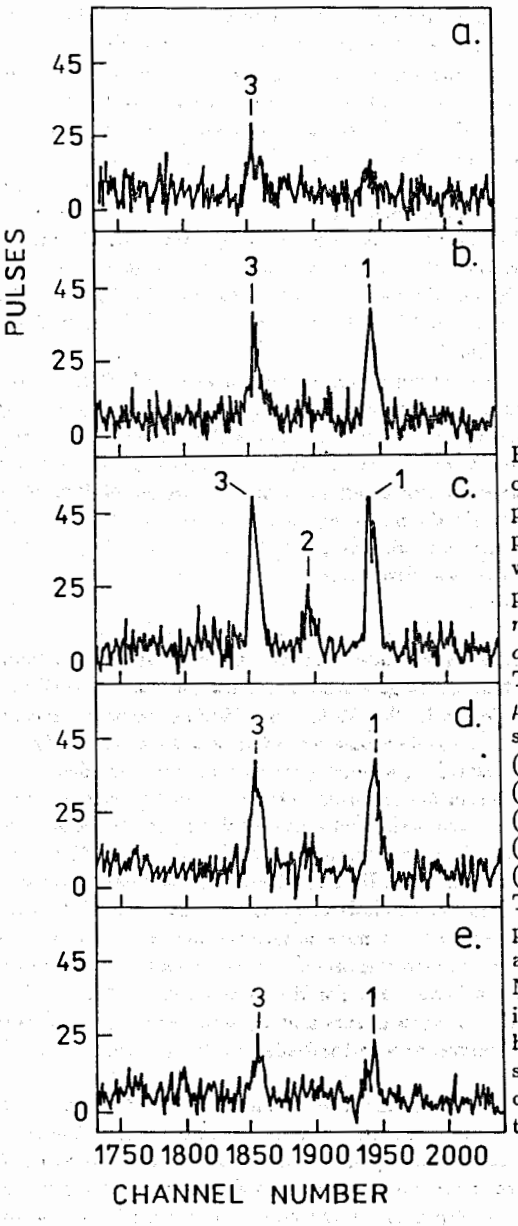

Fig. 13. Diffractograms of the sample of BT6 HTSC material (titanium, α-phase, hexagonal grate) from V3T experiment of April 14, 1992 performed with NSVR of FLNP JINR. The sample is a cylinder with a diameter=8 *mm*, height=20 *mm*, volume V=1 cm^3, and the exposition time, 20 *min*. The time channel width is $\Delta\tau'$=64 μsec. The A detector: 2θ=160°, the scanning net is 7.2°×7.2° (see fig. 4).
(a) the v3t2.a26 spectrum,
(b) the v3t2.a27 spectrum,
(c) the v3t2.a28 spectrum,
(d) the v3t2.a29 spectrum,
(e) the v3t2.a30 spectrum.
The IBR-2 reactor operated in a pulsed mode with a frequency of 5 *Hz* and a mean power of 2 *MW*.
Note that reflex (2) is seen clearly only in the (b) spectrum. This reflex is, however, not seen in the other 649 spectra so, it is most probably an accidental hit. This experiment took a total of 34 hours.

sample environment conditions in the geometrical centre of the detector systems and provide the necessary collimation resolution of the scattered beam with good transmission.

Why do we discuss the spectrometer version which allows the *DM* positioning with the density of 4°? The answer is: the texture analysis of rock samples needs the density of a regular scanning net of not less than 5°× 5°. At the same time test, NSVR experiments investigating HTSC textures have shown that these investigations require a scanning net density of 1°×1°. The proposed NSKAT-55-4 spectrometer would be capable of providing a scanning net density of 1°× 1° at a minimum measuring time.

The above clarifies the meaning of the figures in the name of the spectrometer: 55 means the diameter in *mm* of the transverse cross section of the neutron beam, and 4 means the maximum possible density in (°) of *DM* positioning. According to this classification the NSVR instrument could be given the name of NSKAT-50-14, and the SKAT instrument under construction, the name of NSKAT-50-5.6.

Figures 12 and 13 illustrate the instrumental diffraction spectra of some HTSC small volume samples measured with NSVR. These measurements demonstrated the necessity of using a special detector system to increase the usage efficiency of the beam. The matter is that the sizes of HTSC samples match the 20 *mm* diameter sphere. It is therefore planned to build a BDC90°-20-4 block detector system specially for small samples. The main BDC90°-20-4 dimensions (see fig. 11) will be approximately the following:
R_1= 150 *mm* - the centre of sample to collimator distance,
R_2 = 360 *mm* - the distance to the centre of the detector,
R_3 = 510 *mm*,
R_4 = 610 *mm*.
In the BDC90°-20-4 system, decreasing the R_2 distance by approximately 3.75 times in comparison to the DC90°-55-4 detector system would give a 14 times increase in the scattered neutron flux on the detectors in comparison to DC90°-55-4, and a 19 times increase in comparison to NSVR. For example, it took 15 hours to measure the five spectra shown in fig. 12 with NSVR. The BDC90°-20-4 would allow taking 45 such spectra with the same statistical accuracy and a scanning step of 2° in 20 minutes (with 23 detectors), and with a scanning step of 1° in 40 minutes. In fig. 11 this system is shown to occupy the positions DC20° and DC160°. Such a system can be easily placed inside a ring on the *XY* plane. The DC20° and DC160° positions are the extreme sites at which the BDC90°-20-4 detector system could be placed. In a beam with a 55×200 *mm* cross section all detector systems could be distributed over the beams height to make it possible to carry out measurements simultaneously on three samples. The project assumes vacuumizing the inner space of the spectrometer, as beam loss due to absorption in air is 3% per meter of flight path. For NSVR this loss is 20%.

Equipment for the control of NSKAT type instruments and registration of data has been developed, and is now in the process of construction on the basis of VME-standard at FLNP [11].

The NSKAT-55-4 spectrometer could be installed on beam 14 of the IBR-2 reactor. The beam has not been used for measurements previously. The spectrometer's positioning on beam 14 would provide the possibility of expanding the texture investigation program. In addition, this would most probably permit carrying out control of the state of the movable reflector . The matter is that the reflector passes by the reactor core and beam 14 and shadows them at the moment when the power pulse develops. As a result, any changes in

the state of the reflector's material (radiation swelling or micro-fractures) are reflected in the neutron spectrum. The reflector's state could be checked at the beginning and at the end of each reactor cycle.

NSKAT Equipment Components include:
1. Instrument-carrying structure.
2. Collimators.
3. Detectors.
4. Detector electronics.
5. High-voltage power supply for detectors.
6. Low-voltage power supply for detector preamplifiers.
7. Control and measurement system in VME standard.
8. Goniometers.
9. Auxiliary equipment: teodolite, adjusting laser.
10. Experimental data processing equipment:
a) two sets of PC-486 computers with peripherals;
b) SPARCstation.

6. Discussion on the NSKAT Spectrometer Project for the ET-RR-1 Stationary Reactor

6.1 Dimension estimates of the instrument-carrying structure

Critical parameters of the spectrometer for the ET-RR-1 reactor:
a) transversal cross section of the neutron beam - 13×90 *mm*;
b) centre of beam to floor distance - 1 *m*.

Here, we will give the spectrometer the conditional name of NSKAT-13.

First, we shall consider the issue of the size of samples which could be used in texture investigations on such a beam:
— for a spherical sample, if the maximum diameter accepted is equal to 12 *mm*, then its volume is V=0.9 cm^3;
— for a cylindrical sample, the maximum spatial diagonal is 12 *mm*, then the diameter is 8.5 *mm*, the height is 8.5 *mm*, and the volume is V=0.48 cm^3;
— for a cubic sample, the maximum spatial diagonal is 12 *mm*, the side is 7 *mm*, and the volume is V=0.34 cm^3.

So, the conclusion immediately follows that one cannot investigate textures of geological materials (rock samples) with the NSKAT-13 spectrometer. As it has been said above, to do this one needs to have samples with a volume from 20 to 30 cm^3.

Now, let us consider the question of possible NSKAT-13 dimensions (hereinafter, see fig. 11 for the notations of dimensions and systems). The cross section of the entrance window of FSC is accepted to be 15×15 *mm*. Then the size of such a collimator in the scattering plane should be 35 *mm*. For the given density of 4° DM positioning, R_1 = 500 *mm*. In this case, to use sample environment equipment, e.g., high pressure cells (HPC) during the measuring process, one needs some free space in the centre of the spectrometer. The present level of high pressure technology permits building a 120 *mm* diameter HPC for single-axis compression of 20cm^3 volume samples with the force $F = 1.5 \times 10^5 N$, and for volume compression under the hydrostatic pressure of P=1500 MPa with the possibility of simultaneous single-axis compression with the force F=5×10^4 N of 4 cm^3 volume samples. In texture experiments

the most profitable orientation of the HPC longitudinal axis is at an angle of 45° to the beam axis. Then, with consideration of the FSC size, the necessary and sufficient free space in the scattering plane is determined by R=110 *mm*. In further, we shall discuss the structure of NSKAT-13 with the detector positioning density of 4°, i.e., of the NSKAT-13-4 spectrometer. The main NSKAT-13-4 dimensions are approximately the following (see fig. 11):
for separate DM: $R_1 = 500\ mm$, $R_2 = 750\ mm$, $R_3 = 900\ mm$, $R_4 = 1000\ mm$, $R_5 = 1200\ mm$, $R_6 = 1600\ mm$;
for the BDC90°-15-4 block detector system: $R_1 = 110\ mm$, $R_2 = 260\ mm$, $R_3 = 410\ mm$, $R_4 = 510\ mm$, $R_5 = 700\ mm$, $R_6 = 900\ mm$.

6.2. Choice of the resolution and chopper for the NSKAT-13-4 spectrometer

For the convenience of comparison, let us choose the resolution R=0.7%, i.e., the same as the NSVR resolution for the inter-planar spacing $d = 2\AA$ at 2Θ=90°.

The resolution of the spectrometer, $R=\Delta Q/Q$, at a pulsed neutron source (without a chopper) is determined by the formula [9]:

$$\Delta Q/Q = [(\Delta t/t)^2 + (\Delta L/L)^2 + (ctg\Theta \times \Delta\Theta)^2]^{1/2}, \qquad (11)$$

where $\Delta t(\lambda) = (m/\hbar)\lambda\delta_m$ is the uncertainty related to the moderation time; $\delta_m \simeq \Delta L$ is the effective uncertainty accepted to be equal to 28 *mm* in simpler calculations.

To build a diffractometer with optimal parameters, i.e,, to achieve the maximal intensity for the given resolution, calculations are performed under assumption that all the terms entering formula (10) are independent and equal to each other. Then we have:

$$\Delta t/t = \Delta L/L = ctg\Theta \times \Delta\Theta = R/\sqrt{3}. \qquad (12)$$

To choose the total flight path we take the resolution equal to R=0.4%, i.e., to the best NSVR resolution. Then from (11) we obtain:

$$L = \delta_m\sqrt{3}/R \simeq 12\ m. \qquad (13)$$

To stage a time-of-flight experiment at a stationary reactor it is necessary to use a neutron beam chopper. The resolving power, R_0, of a diffractometer with a chopper, regardless of neutron wavelength, is

$$R_0 = d\tau/L = (\Delta\tau + \Delta\tau')/L, \qquad (14)$$

where $\Delta\tau$ is the duration (μsec) of the pulse transmitted by the chopper, $\Delta\tau'$ is the time width of the counting channel (μsec) for detection, and L is the total flight path (mm).

The detecting conditions are optimal for $\Delta\tau$=$\Delta\tau'$. Let us take $\Delta\tau'$= 64 μsec as in the NSVR experiments. Then, $d\tau$=128 μsec and

$$R_o = 0.01 = 1\%.$$

As a result, for the interplanar spacings d=2Å the resolution should be $R_d = \Delta d/d$=0.007=0.7%, i.e., the same as for NSVR.

Let us consider the possibility of using three types of choppers: disc, rotor (Fermi), and correlation (Fourier).

We shall limit the NSKAT-13-4 working range to the interval of interplanar spacings Δd=0.05 - 0.4 (nm), or correspondingly, to the wavelength interval of the primary beam

$\Delta\lambda$=0.07-0.57 nm, which is quite sufficient for investigating the majority of crystalline materials. The minimum neutron velocity for this interval is v=0.7 $mm/\mu sec$. The pulse frequency of the chopper should be f=1/(12000/0.7)×10⁶=58 p/sec to prevent the overlapping of pulse periods. A disc chopper with one slit 13 mm wide and 90 mm long should have a radius of 570 mm and rotate at a speed of 3480 rot/min for $\Delta\tau = 64\ \mu sec$. Then, the linear velocity at the disc periphery will be 208 m/sec, which is quite acceptable because the limit velocity for the majority of materials is 400 m/sec. We have chosen the slit width of 13 mm to keep the maximal beam area. This would give the possibility of having a maximum beam intensity when using crystal monochromators if it should be necessary to measure exactly one individual peak.

To carry out a comparative analysis of scattered beam intensities on NSKAT-13-4 and on BDC or NSVR, we accept that the neutron beam of the ET-RR-1 reactor with a 12 m mirror neutron guide and a cross section of 13×90 mm without a chopper has an exit flux of $1\times10^7\ n/cm^2s$ (we know that this reactor has a 20 m beam with such parameters). The neutron flux at the exit of the NSVR neutron guide is $1.2\times10^6\ n/cm^2s$. The disc chopper with the chosen parameters would reduce the flux by 360 times. The intensity gain achieved by positioning the detectors closer to the sample than in NSVR would be by a factor of 37. So, the times for measuring the same volume samples should be practically the same.

The Fermi-chopper would limit the wavelength interval.

The Fourier chopper would enable a 50% transmission, but the appearance of a correlation background (lost information background) would further reduce the luminosity of the diffractometer [12].

6.3. A program of possible investigations with NSKAT-13-4

The NSKAT-13-4 spectrometer could be used to solve the following scientific-research problems (for comparison, see Section 4.1):

2. Investigations of the dynamics of texture changes in metal and metal alloy samples under the influence of external conditions modifying the textures directly in the neutron beam. Simultaneous measurements of internal stresses in these samples.

3. The same as 2 with samples of polycrystal, ceramic, and polymer materials of artificial origin (homogeneous in composition).

4. Measurements of the texture of HTSC materials to elaborate techniques for producing HTSC's.

7. Conclusion

Analysis of material textures gives valuable scientific information and helps solve fundamental and applied problems in the field of condensed matter physics.

Here we propose to use the time-of-flight method in neutron diffraction investigations of material textures at the ET-RR-1 type reactor or at an even more powerful reactor.

The proposed version of the spectrometer does not depend on the type of neutron beam chopper (disc, Fermi-, or Fourier-chopper). This spectrometer would also allow the use of crystal monochromators.

The possibility of choosing the spectrometer mode, i.e., with a chopper or a monochromator, gives experimentalists the freedom to choose their experimental techniques, and at the same time, poses the problem of developing electronic equipment to control the instrument

and devices for data registration. FLNP JINR has experience in developing and manufacturing such electronic systems both for pulsed and stationary reactors.

Acknowledgements

Thanks to T.F.Drozdova for the English translation.

References

1. G.Vasserman, I.Greven. Textures of Metal Materials. M., "Metallurgy", 1969 (in Russian).

2. Ya.D.Vishnyakov, A.A.Babareko, S.A.Vladimirov, I.V.Egiz. The Theory of Texture Formation in Metals and Alloys. M., "Nauka", 1979 (in Russian).

3. User Guide, Neutron Experimental Facilities at JINR, Dubna, 1992, 17-18.

4. K.Walther, K.Helming, W.Voitus. The SKAT Spectrometer for Quantitative Analysis of Textures (Project), FLNP JINR, Dubna, 1989.

5. K.Walther, N.N.Isakov, A.N.Nikitin, K.Ullemeyer, J.Heinitz. Progress in Texture Investigations at NSVR of LNP. JINR-FRG Cooperation in Neutron Physics. Results of 1992 and Plans for 1993, Dubna 1992.

6. W.Voitus, J.Heinitz, K.Walther, N.N.Isakov. Neutronographisce Bestimmung von Polfiguren am Diffraktometer NSVR im VIK Dubna. Arbeitstreffen des Verbundes "Forschung mit Neutronen", 29.03-01.04.1992. in Bad Schndau.

7. K.Walther, N.N.Isakov, A.N.Nikitin, K.Ullemeyer, J.Heinitz. Texture Investigations of Geomaterials by Diffraction Methods with the High Resolution Neutron Spectrometer in FLNP JINR. The Physics of the Earth, 1993, No.6, p. 37-44 (in Russian).

8. K.Helming. The Method of Geometrical Approximation for Texture Analysis of Rocks. The Physics of the Earth, 1993, No.6, p.73-82.

9. K.Windsor. Neutron Scattering at Pulsed Sources. M., "Energoatomizdat", 1985 (in Russian).

10. N.Popa. The Resolution Function in Neutron Diffractometry. JINR, P14-87-293, Dubna, 1987.

11. Zen En Ken, N.N.Isakov, A.S.Kirilov, M.L.Korobchenko, A.I.Ostrovnoj, V.E.Rezaev, A.P.Sirotin, J.Heinitz. A VME System for data collecting and control of the NSVR spectrometer. JINR, P13-94-73, Dubna, 1994.

12. V.L.Aksenov, et al. The Fourier Neutron Diffractormeter at the IBR-2 Reactor. JINR, P3-91-172, Dubna, 1991 (in Russian).

Received by Publishing Department
on July 6, 1995.